https://doi.org/10.48048/tis.2024.7261

Analysis of Pneumonia Area Development in Covid-19 Patients based on Sequential X-Ray Images Using the Seq_UB Architecture

Chomsin Sulistya Widodo[1,*], Agus Naba[1], Yuyun Yuewniwati[2] and Muhammad Masdar Mahasin[1]

[1]Department of Physics, Faculty of Mathematics and Natural Science, Brawijaya University, Jawa Timur 65145, Indonesia
[2]Department of Radiology, Faculty of Medicine, Brawijaya University, Jawa Timur 65145, Indonesia

([*]Corresponding author's e-mail: chomsin@ub.ac.id)

Received: 1 July 2023, Revised: 24 July 2023, Accepted: 25 July 2023, Published: 30 October 2023

Abstract

Introduction
During the covid pandemic, radiologists diagnosed covid patients by analyzing chest X-ray images. The existence of a quantitative system can help visual observation of lung conditions by radiologists.

Purpose of research
This research aims to develop an image segmentation algorithm, Seq_UB, which can monitor the development of the lung condition of Covid-19 patients periodically. The Seq_UB algorithm was developed by modifying the UNet system using different CNN layers according to the UBNet v1 algorithm.

Materials and methods
The dataset for training uses the Montgomery USA Dataset, which contains 138 CXRs with a resolution of 4,020×4,892, of which there are 80 normal CXR images and 58 CXR images of patients identified with tuberculosis; the Shenzhen Hospital Dataset consists of 662 CXR images, of which there are 336 abnormal CXR images.

Result and discussion
The results show that reducing the input image size does not significantly affect the accuracy of the segmentation results. However, reducing the input image size will affect the resolution of the segmentation results. Where the smaller the input image size, the lower the resolution obtained. This will have an impact on the final interpretation of the segmentation results. Research shows that an input image size of 512 is the best because the resolution of the segmentation results is still very accurate. This study shows that the Seq_UB architecture can perform X-ray image segmentation with relatively stable accuracy and lower computational burden. An interesting pattern was found, where Covid-19 patients quantitatively experienced fluctuations in image segmentation size.

Conclusions
The Seq_UB system can perform well with a segmentation accuracy of 96 %, and the processing speed takes 0.91 s. A desktop GUI was designed to segment X-ray images more effectively.

Keywords: Deep learning, Segmentation, X-Ray, Pneumonia, Covid-19

Introduction

Early diagnosis of the condition of Covid-19 patients is needed to monitor the condition of Covid-19 patients quickly and accurately so that appropriate treatment can be carried out. Radiologists use chest X-rays to diagnose and monitor the condition of the lungs of Covid-19 patients [1]. Research shows that most Covid-19 patients with severe symptoms also have pneumonia. Inside the lungs, the fluid disrupts the respiratory system, making it dangerous for patients and can lead to death [2]. Research shows that Covid-19 causes inflammation in the lungs of patients to different degrees. A recent study showed that Covid-19 patients who have recovered within a certain period still have residual abnormalities based on Chest X-Rays (CXR) images of the patient's lungs [3]. Analysis of chest X-ray images of Covid-19 patients is currently carried out manually by radiologists so that the results of diagnosis and study also depend on the experience and expertise of each radiologist because they are qualitative [4]. So a method is needed for the quantitative analysis of X-ray images.

Image processing methods are used in X-ray image analysis, including medical image processing, which has developed significantly with both artificial intelligence and conventional methods such as k-means clustering, ROI-based segmentation, and watershed techniques. [5]. Many studies have discussed the application of these methods for medical image purposes. Some of the image processing applications that have been developed include eye retina images, X-ray images, EEG signals, and CT-scan images [6].

Along with the development of science and technology, research on artificial intelligence-based image segmentation methods has also been developed using Artificial Neural Networks for medical physics [7]. In general, the application of artificial intelligence in image processing includes image classification [8], image detection [9], image segmentation [10] and image generation based on Generative Adversarial Networks [11]. In its application in the medical world, image segmentation methods are needed in the case of X-ray image segmentation. Such as cancer segmentation for radiotherapy purposes, brain tumor segmentation to determine the extent of the tumor, and lung segmentation to estimate the area of the lungs affected by pneumonia.

Previous research has been conducted by developing convolutional neural networks (CNN)-based segmentation architectures such as SegNet, FCN-8, FCN-32 and standard Unet. The accuracy of the previously developed methods was still relatively low at +75 % and did not consider the computational burden in the development of the architectures. A recent study in Nature has evaluated several image segmentation models for CXR images [12]. The comparison included key factors such as input size, total parameters, and dice similarity coefficient (DSC) values. The models compared in this study included UNet++, DeepLabV3, DeepLabV3+, FPN, LinkNet, PSPNet, PAN and MA-Net. This research provides valuable insights into the performance and efficiency of different models for CXR image segmentation and can help select the most appropriate Model for a particular application. However, it is important to note that there is still a need to develop lightweight and accurate models for CXR image segmentation to improve the performance and efficiency of this task.

This study developed a deep learning model for opacity segmentation in X-ray images of Covid-19 patients by modifying the UNet CNN architecture [13]. The modification is done by rebuilding the UNet architecture based on the lightweight UBNet image classification architecture [14]. UBNet is explicitly developed to process lightweight X-ray images in the case of image classification. Standard UNet segmentation results without modification were used as a comparison in validating the segmentation model in terms of model load, execution time, and model accuracy. After developing a lightweight and accurate model for CXR image segmentation, the next step is integrating it into a system for quantitative analysis of Covid-19 CXR images. This system will be able to analyze images, extract relevant information, and quantitatively monitor the progression of Covid-19 based on CXR images. This system will enable more accurate and efficient disease tracking and can assist in developing more effective treatment and management strategies. In addition, the system can be integrated with existing healthcare systems and used by radiologists and other medical professionals to monitor patient disease progress.

Materials and methods

Dataset

The datasets used are open data that institutions have published in previous studies, including (1) Montgomery USA Dataset, which contains 138 CXRs with a resolution of 4,020×4,892 of which there are 80 normal CXR images and 58 CXR images of patients identified with tuberculosis; (2) Shenzhen Hospital Dataset consisting of 662 CXR images, of which there are 336 abnormal CXR images. This dataset contains the original X-ray image of the patient and the result of manual segmentation. The X-ray image is used as the model input, and the manual X-ray segmentation is used as the model target during training. So the total dataset used is 800 CXRs [15-18].

Seq_UB architecture

In this research, a modified UNet image segmentation method has been developed. The UNet image segmentation method was introduced in mid-2015 in a journal by Olaf Ronneberger *et al.* (2015). U-Net is an extension of the Fully Convolutional Networks (FCN) Semantic Segmentation method published in early 2015. The basic concept of UNet can be modified according to the needs [13,19]. In the UNet architecture, a convolution layer with a size of 3×3 is used by default in every setup. The UNet architecture is designed and trained in Python with TensorFlow [20], and Keras [21].

The designed image segmentation architecture has a structured pattern similar to UNet, but the arrangement of convolution layers is different. The UNet modification changes the layer arrangement according to the UBNet v1 architecture. Then, the layers are arranged on the next side in reverse order, referred to as a mirror. Thus, the modified UNet architecture refers to the UBNet structure developed in previous research. The visualization of the Seq_UB segmentation architecture is shown in **Figure 1**. Seq_UB has a more straightforward architecture design compared to the general UNet architecture design.

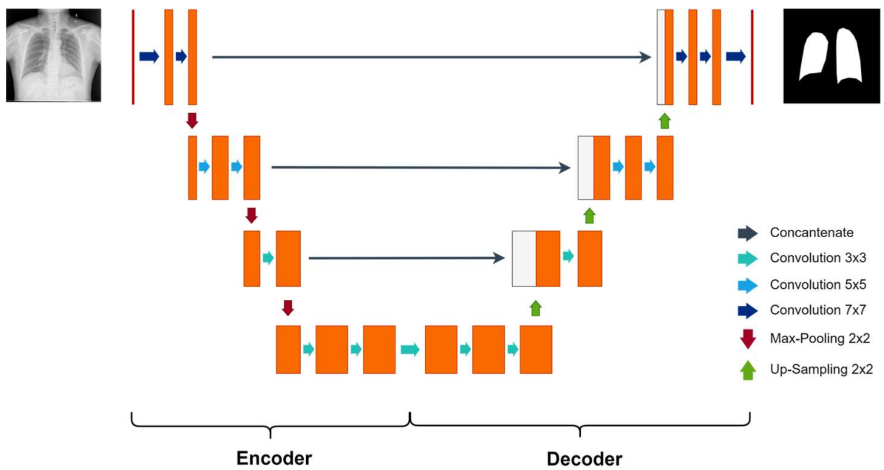

Figure 1 Seq_UB image segmentation architecture.

The use of different layer arrangements in Seq_UB impacts other characteristics of the segmentation result and the number of parameters involved. UBNet was developed to obtain a lightweight, fast architecture for processing chest X-ray images. The total parameters of Seq_UB are lower than UNet. A comparison of the total parameters of UNet and Seq_UB is shown in **Table 1**.

Table 1 Total parameters of UNet and Seq_UB.

Architecture	Total parameter
UNet	7,759,521
Seq_UB	2,379,073

The total parameter value of Seq_UB, when compared to UNet, shows a significant decrease of about 3 times. It is assumed that this can reduce the computational burden when performing the image segmentation process. The decrease in the total parameter value is due to the different arrangements of convolution layers and the different parameters in each convolution layer.

Evaluation

The main parameters in evaluating the Seq_UB model are model accuracy and model efficiency. The accuracy of the Model is assessed based on the Dice Coefficient value. In contrast, model efficiency is evaluated by reviewing the average execution time and size of the Model when stored in the .h5 extension. Testing the accuracy of the UNet - UBNet model uses the Dice Coefficient metric.

Dice Coefficient indicates how accurate the predicted mask of the detection performed by the Model is to the actual image mask in the dataset, commonly referred to as ground truth. The larger the Dice Coefficient value, the better the Model. Meanwhile, the smaller the Dice Coefficient value, the better the Model is interpreted. The value of the Dice Coefficient is between 0 and 1. A value of 0 is an inaccurate interpretation of the segmented image to the ground truth.

Conversely, a value of 1 means that the segmented image is the same as the ground truth. So we will compare the evaluation results of Seq_UB with the Dice Coefficient values of the models created in previous studies, including UNet, SegNet, and FCN. Dice Coefficient calculation can be done with equation;

$$DSC\ (X, Y) = \frac{2\ |X \cap Y|}{|X| + |Y|} \tag{1}$$

Model efficiency is evaluated by calculating the average execution time for each UNet and Seq_UB model trained to segment X-ray images of Covid-19 patients; the less time it takes to perform segmentation, the higher the model efficiency. Then the efficiency of the Model is also reviewed based on the Model's size that has been trained. The smaller the model size, the less storage space is required on the hardware. Smaller models are also more likely to be used on lower hardware and internet hosting.

Covid-19 CXR development monitoring system

The trained Seq_UB model is then stored in .h5 format. This Model is used to build a monitoring system for developing X-ray images of Covid-19 patients [22]. Since the available data of sequential chest X-ray images of Covid-19 patients is limited, research was conducted on data obtained in open journals. This analysis was carried out to observe the development pattern of the lung condition of Covid-19 patients based on changes in opacity in the chest X-ray images of Covid-19 patients. They measured the percentage of lungs quantitatively. This is done by comparing the segmented image with the average segmented area of the normal patient's lung image. The approximate calculation of the percentage of segmented lungs is;

$$\text{Percentage CXR} = \frac{\text{segmented CXR input}}{\text{normal CXR segmentation}}\ X\ 100\% \tag{2}$$

The Covid-19 patient X-ray image monitoring system was also developed as a Graphic User Interface or can be abbreviated as GUI, which aims to facilitate users in analyzing new chest X-ray images. This GUI is written in Python using the PyQt5 library. The GUI is run on a local computer and uses a pre-trained Seq_UB model. The GUI will display 3 primary columns. The first column displays the chest X-ray image, which will be analyzed using the Seq_UB model. The second column displays the analysis results in the form of the patient's chest X-ray image and the segmentation results based on the Seq_UB model analysis. The third column displays a summary of the diagnosis results.

Results and discussion

Comparison of UNet and Seq_UB segmentation accuracy

After the Seq_UB architecture is built, the following process is to train and test the dataset. The training process is performed in up to 100 iterations. However, the process is also set to stop training when there is no additional performance to avoid model accuracy degradation and over-fitting. Different input size variations were performed on the UNet and Seq_UB architectures. The input variations used are 128×128, 256×256 and 512×512. After training, the accuracy values during training were obtained. The graph of UNet training with various inputs is shown in **Figure 2**.

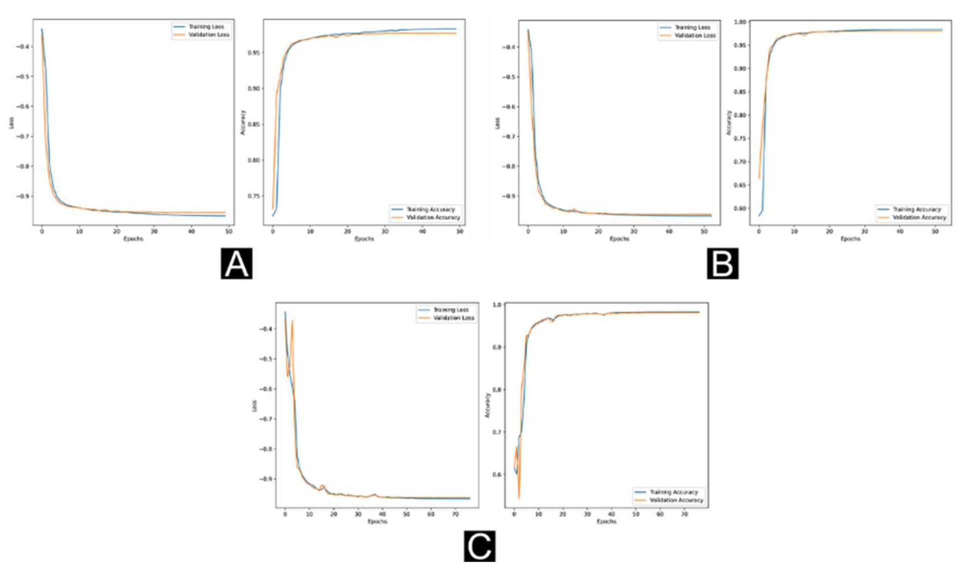

Figure 2 UNet training graph with inputs; (a) 128×128, (b) 256×256 and (c) 512×512.

Based on the UNet training graph in **Figure 2**, the accuracy of the UNet model for segmentation shows good results above 95 %. Changing the input image size does not affect the accuracy value in this training. However, it should be noted that the total UNet parameters are quite large, reaching 7,759,521. Next, the Seq_UB architecture was trained. The training graph is shown in **Figure 3**.

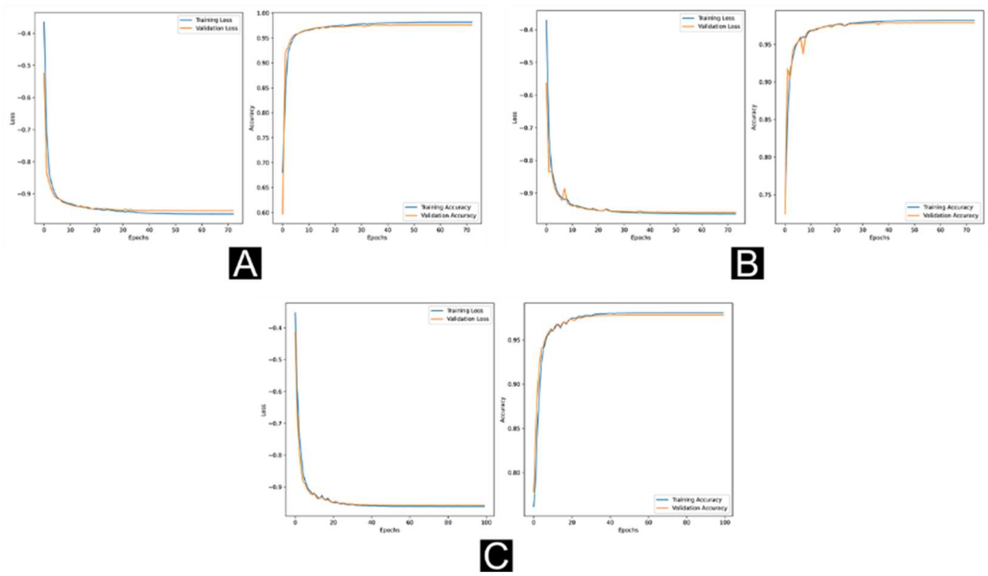

Figure 3 Seq_UB training graph with inputs; (a) 128×128, (b) 256×256 and (c) 512×512.

The graph in **Figure 3** shows that the training accuracy of the Seq_UB model also shows good accuracy with values above 95 % for different input variations. Seq_UB shows it can segment well even though its total parameters are 3 times lower than the UNet architecture. Changing the input size will impact the visual appearance of the segmented image. The smaller the input, the coarser the resulting image. Meanwhile, the larger the input size, the smoother the resulting image will be. The visualization of the UNet output with various variations is shown in **Figure 4**.

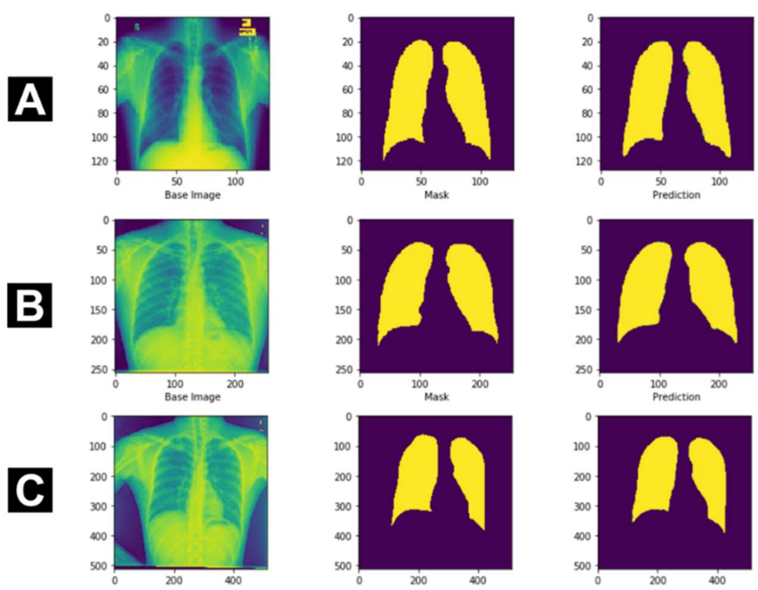

Figure 4 Visualization of UNet segmentation results with inputs; (a) 128×128, (b) 256×256 and (c) 512×512.

This study also compares the performance of Seq_UB and UNet to segment CXR images. The segmentation results in **Figure 5** show that both architectures produce results similar to the ground truth. Although both Seq_UB and UNet can achieve good CXR segmentation, Seq_UB has a more straightforward convolution layer arrangement and a lighter computational load than UNet. This system suggests that Seq_UB may be a more efficient or easier-to-implement solution for CXR image segmentation while still performing similarly to UNet.

The evaluation results in **Table 2**. show that the Dice Coefficient value of the Seq_UB architecture is relatively similar to the UNet architecture for several different input sizes. This indicates that the Seq_UB image segmentation architecture design has promising results, with the total parameters up to 3 times lower than the UNet architecture.

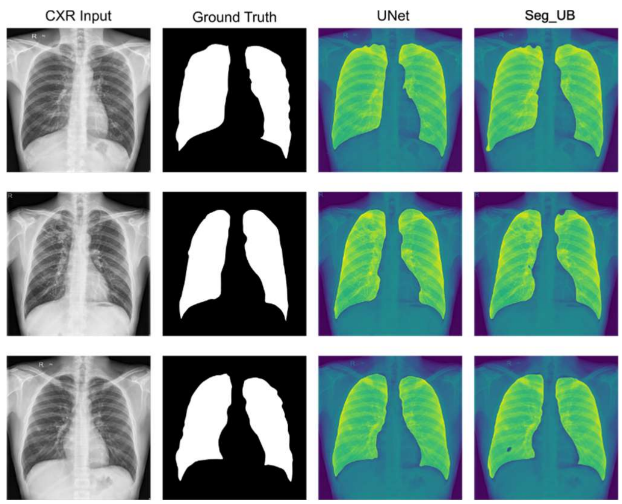

Figure 5 Comparison of Segmentation Results with Seq_UB and UNet.

Table 2 Dice Coefficient of UNet and Seq_UB.

Architecture	Total parameter	Size 128	Size 256	Size 512
UNet	7,759,521	0.9548	0.9609	0.9626
Seq_UB	2,379,073	0.9527	0.9585	0.9577

Comparison effectiveness of UNet and Seq_UB

When viewed from the total parameters, the total parameters of Seq_UB are 3 times less than the total parameters of UNet. So it can be interpreted that the computational process on the Seq_UB architecture is lighter than the UNet architecture. The trained Model is saved in .h5 format and then used to build the segmentation GUI. Based on the memory model size, it is found that Seq_UB is lighter than standard UNet by +70 %. The size of the pre-trained UNet model is 91 MB, while the size of Seq_UB is only 28 MB. So Seq_UB is more potential to be applied in cloud computing. Then analyze the difference in segmentation time between UNet and Seq_UB models by taking the average time. By using the UNet and Seq_UB models, the segmentation time data obtained are shown in **Table 3**. The average segmentation time of UNet is 1.13 s. In comparison, Seq_UB takes an average time of 0.91 s.

Table 3 Comparison of UNet and Seq_UB segmentation times.

Model	Segmentation time(s)						Average time(s)
	1	2	3	4	5	6	
UNet	1.53	1.05	1.06	1.06	1.05	1.05	1.13
Seq_UB	1.15	0.86	0.85	0.87	0.86	0.85	0.91

Segmentation time testing was also conducted with the input image of a 59-year-old man from **Figure 11**. The segmentation time results of the UNet and Seq_UB models are shown in **Table 4**. The average segmentation time of UNet is 1.14 s. At the same time, Seq_UB takes an average time of 0.91 s. Based on comparing the time required in the input image segmentation process with the UNet and Seq_UB models, it can be concluded that the Seq_UB model takes +20 % faster than the UNet model.

Table 4 Comparison of UNet and Seq_UB segmentation times.

Model	Segmentation time(s)						Average time(s)
	1	2	3	4	5	6	
UNet	1.56	1.04	1.03	1.05	1.14	1.04	1.14
Seq_UB	1.15	0.86	0.88	0.86	0.85	0.85	0.91

Monitoring CXR opacity changes with Seq_UB

The Seq_UB model has been trained and evaluated. Then this Model can be used for image segmentation with new input. Therefore, this Model can be used to monitor the progress of the lung condition of Covid-19 patients. It is expected that by utilizing the segmentation method for monitoring the development of the lung condition of Covid-19 patients, information related to the development pattern of the lung condition of Covid-19 patients can be obtained quickly and accurately.

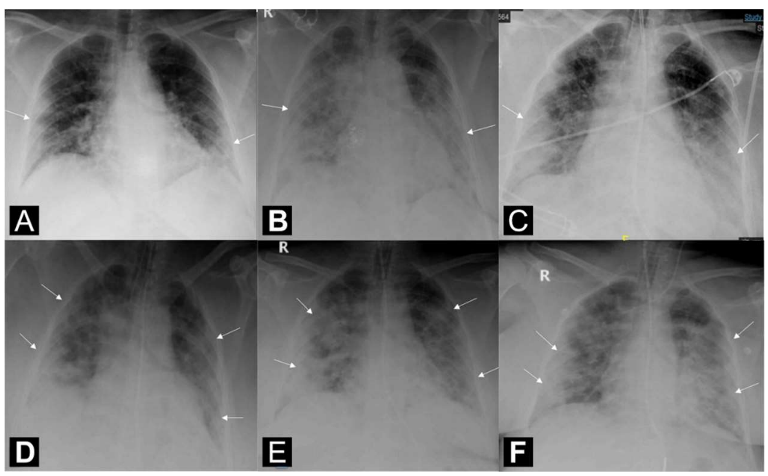

Figure 6 X-ray image data of a 59-year-old female Covid-19 patient [22]. Initial x-ray (a) day 3, (b) day 5, (c) day 7, (d) day 9, (e) day 11, and (f) The patient passed away on day 13.

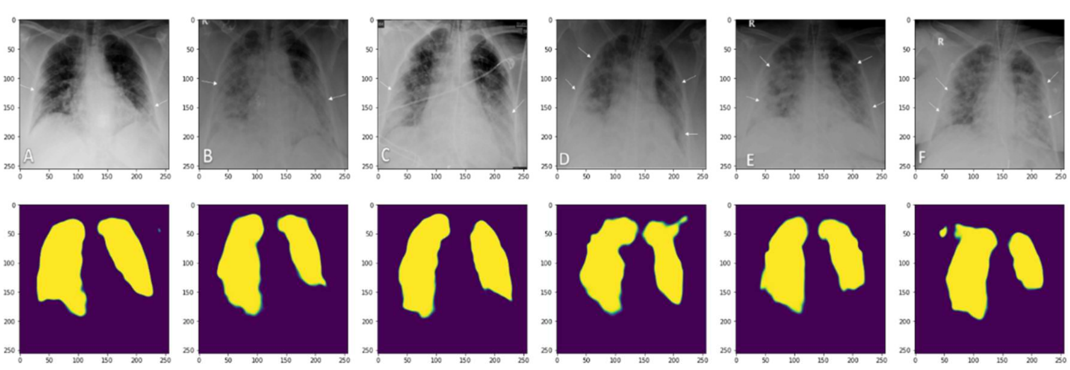

Figure 7 Results of sequential chest X-ray image segmentation (bottom) of a 59-year-old female Covid-19 patient CXR images (top).

Based on the data obtained regarding consecutive chest X-ray images of Covid-19 patients, a segmentation process is carried out for each image. Then the calculation of the estimated lung size in percentage is based on the reference size of the X-ray image of the normal lung so that the percentage value of the remaining lung size will be obtained. **Figure 6**. shows chest X-ray image data of a 59-year-old female Covid-19 patient. Based on the sequential X-ray image data shown in **Figure 7**, a segmentation process is carried out using Seq_UB. The segmentation results of the entire image in **Figure 6**. are shown in **Figure 7**. Then the percentage of the patient's lung area is estimated.

Quantitative measurement of lung estimation is done using Eq. (2). This can be done by calculating the results of image segmentation and normal image segmentation based on the image matrix. In addition, it can also be done by calculating the total pixel value of the segmented image, then comparing it with the average total pixel value of the normal X-ray image segmentation. The total pixel value of the normal X-ray image segmentation is calculated, and the average total pixel value for the normal image is obtained. Then the estimation of the percentage of lung area from the segmentation results with Eq. (2). is based on the average pixel value attached in **Table 5**.

Based on the estimation results of the patient's lung area shown in **Figure 8**, the pattern of the patient's lung condition development can be seen. The condition was quite bad when the patient first entered the hospital and was X-rayed for the first time. Then it gradually improved along with the treatment in the hospital. Until the 6 x-ray, the lung condition worsened, and the patient was declared dead. The lung condition was monitored for the second patient, a 59-year-old man with Covid-19. The X-ray image is shown in **Figure 8**. Segmentation was performed for the patient's chest X-ray image. The segmentation results are shown in **Figure 9**.

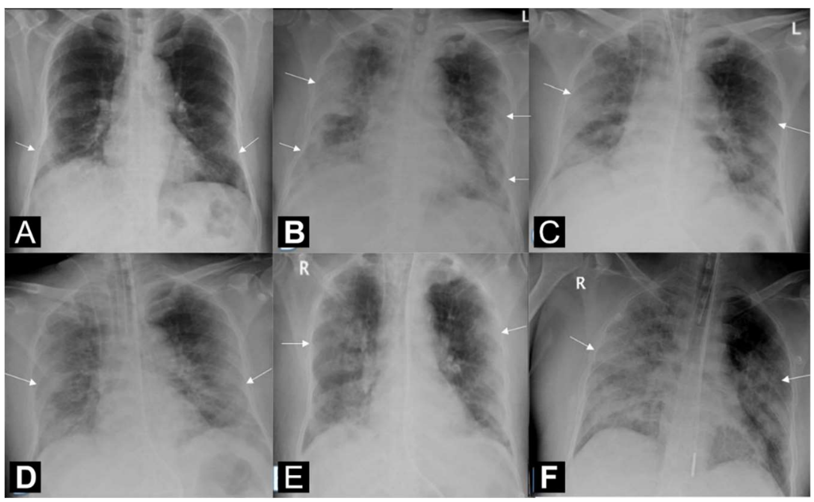

Figure 8 X-ray image data of a 59-year-old male Covid-19 patient [22]. Initial X-ray (A) day 3, (B) day 5, (C) day 6, (D) day 9, (E) day 11, and (F) The patient passed away on day 11.

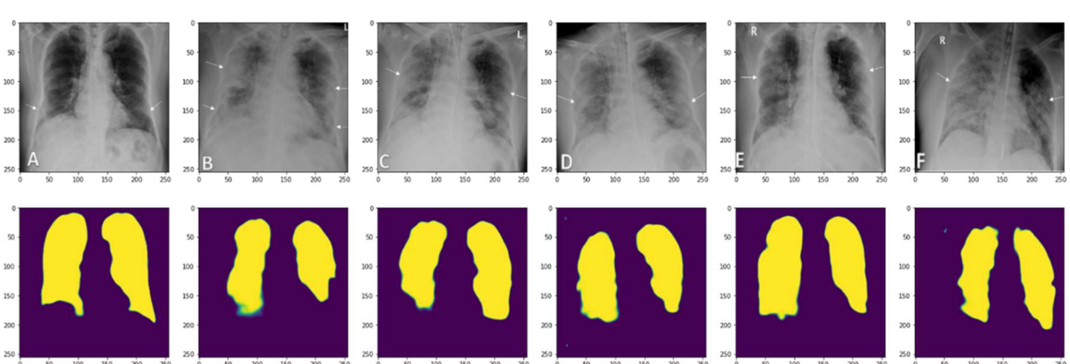

Figure 9 Results of sequential chest X-ray image segmentation (bottom) of a 59-year-old male Covid-19 patient CXR images (top).

Based on the segmentation results in **Figure 9**, the estimated segmented lung size is calculated. The results of this lung segmentation estimation describe the pneumonia condition that occurs in the patient's lungs. The graph of the estimated lung size is shown in **Figure 10**.

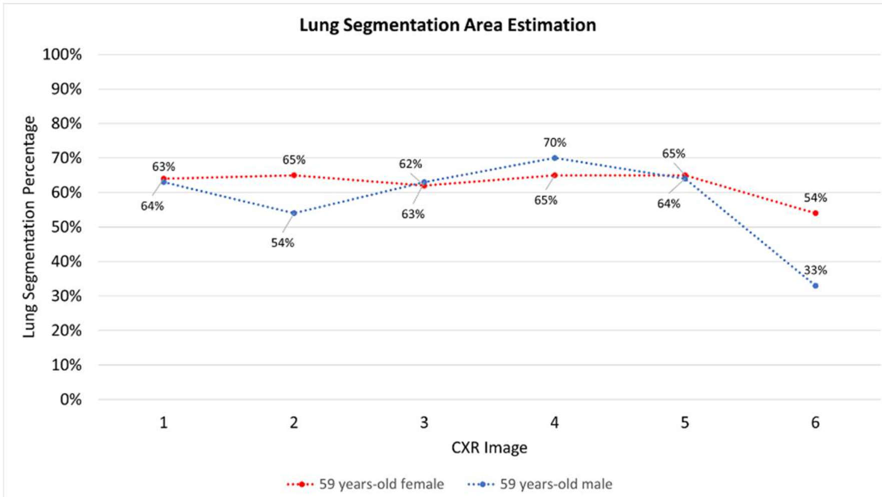

Figure 10 Segmented lung area estimation.

Based on the lung size estimation shown in **Figure 10**, both patient gradually improved during the treatment process. However, in the next condition, the segmented lung size decreased drastically. This can be interpreted that the patient's condition worsened until he was declared dead. Based on the patterns in **Figure 10**, it can be seen that there is a significant relationship between the decrease in segmented lung size and the patient's health condition. The smaller the segmented lung size, the worse the pneumonia condition in the patient's lungs.

Covid-19 CXR segmentation GUI

In its application, it is necessary to create a graphical user interface or GUI to facilitate the use of models and methods in this study to process new X-ray images. The GUI of this chest X-ray image analysis system was created entirely using the Python programming language. This GUI was created as a desktop GUI that can be run on Windows software. The developed GUI consists of 4 pages. The first page is shown in **Figure 11(A)**, which accesses the X-ray image data stored in the database.

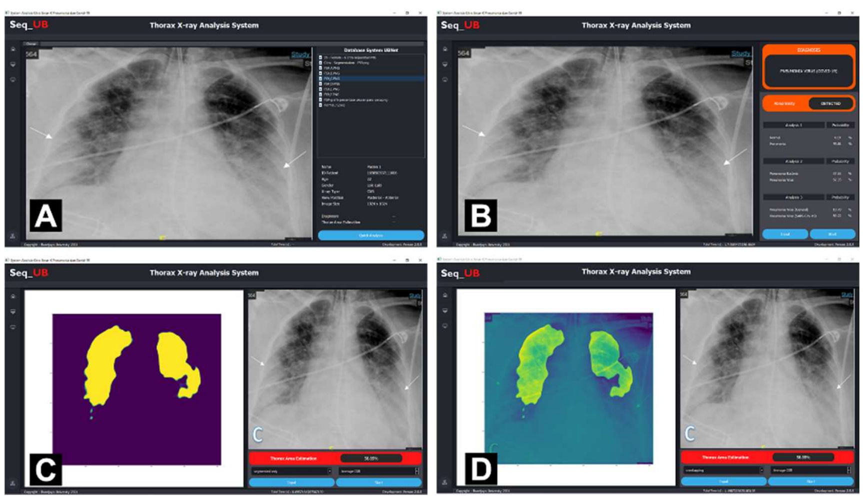

Figure 11 CXR image analysis software display based on Seq_UB; (A) Database page, (B) Second page GUI for patient disease classification, (C) The segmentation page displays the CXR segmentation results, (D) Displays the overlapping CXR segmentation results.

The second page contains the X-ray image classification system for patient diagnosis based on X-ray images, as shown in **Figure 11(B)**. The third page contains the image segmentation system and a column to calculate the estimation of the detected lung area. This research focuses on this third page. The segmentation system consists of a trained Seq_UB architecture model. **Figures 11(C) - 11(D)**. Shows the segmentation system in use.

In **Figures 11(C) - 11(D)**, there are 2 columns of images. On the right is the display of the input image selected for segmentation. The left column displays the segmentation result based on the input image. A red column shows the approximate percentage of the segmented lung size. The 'segmented only' display option is shown in **Figure 11(C)**. Then **Figure 11(D)**. shows the segmentation result display with the 'overlapping' display option.

Discussion

In the medical world, segmenting X-ray images is difficult and time-consuming for radiologists. In the case of Covid-19, segmenting the patient's X-ray images can show the specific condition of the Covid-19 patient's lungs. This allows radiologists to diagnose the lung condition of Covid-19 patients quantitatively. In its application, the segmentation process of X-ray images of Covid-19 patients uses a deep learning algorithm. This research develops an image segmentation architecture to obtain a lighter but more accurate image segmentation architecture. The UNet image segmentation architecture is modified by changing the layer arrangement to resemble UBNet [14]. UBNet is a CNN architecture developed explicitly to process chest X-ray images of pneumonia and Covid-19 patients. UBNet is characterized by simple layer arrangement, high accuracy, and low computational load, so the modification of UNet based on the structure of UBNet allows the construction of a lighter and still accurate image segmentation architecture.

Several image segmentation architectures have been developed, which are shown in **Table 5**. Some studies, such as FCN, SegNet, and UNet, have shown relatively low evaluation values [23]. Of course, this also depends on the number of datasets used. This study compared the Dice Coefficient values between the standard UNet architecture and Seq_UB with different input image sizes. The results show that reducing the image size does not significantly affect the Dice Coefficient value. This means that reducing the input image size does not significantly affect the accuracy of the segmentation results. However, reducing the input image size will affect the resolution of the segmentation results. Where the smaller the input image size, the lower the resolution obtained. This will have an impact on the final interpretation of the segmentation results. The results show that an input image size of 512 is the best because the resolution of the segmentation results is still very accurate [23]. A recent study in Nature compared various image segmentation models for CXR images. Including input size, total parameters, and DSC values [12] **Table 6**. Shows a comparison of the input image size, total parameters, and DSC values of several CXR image segmentation models. Interesting results are obtained, where Seq_UB with input sizes varying from 128, 256 and 512 shows much lower total parameter values than other models. The DSC values for the comparison models in this study were determined based on the best hyperparameter configurations previously reported in the literature.

Table 5 Comparison of several image segmentation architectures.

Network	Modality	Subjects (n)	Mean DSC
UNet[21]	CXR	758	0.74
FCN-32[21]	CXR	758	0.543
FCN-8[21]	CXR	758	0.707
SegNet[21]	CXR	758	0.734
UNet (proposed)	CXR	800	0.963
Seq_UB (proposed)	CXR	800	0.958

The results show that reducing the image size does not significantly affect the Dice Coefficient value. This means that reducing the input image size does not significantly affect the accuracy of the segmentation results. However, reducing the input image size will affect the resolution of the segmentation results. Where the smaller the input image size, the lower the resolution obtained. This will have an impact on the final interpretation of the segmentation results. Research shows that an input image size of 512 is the best because the resolution of the segmentation results is still very accurate [23].

Table 6 Comparison parameter, input size, and DSC with several models.

Model	Input size	Parameter (Million)	DSC
UNet++ [24]	384	9.1	0.946
DeepLabV3 [25]	512	7.3	0.938
DeepLabV3+ [26]	512	7.4	0.948
FPN [27]	544	5.8	0.949
LinkNet [28]	480	29.3	0.946
PSPNet [29]	480	29.7	0.94
PAN [30]	512	4.1	0.941
MA-Net [31]	512	13.4	0.945
Seq_UB (proposed)	128	2.38	0.953
Seq_UB (proposed)	256	2.38	0.959
Seq_UB (proposed)	512	2.38	0.958

This study shows that the Seq_UB architecture can perform X-ray image segmentation with relatively stable accuracy and lower computational burden. Seq_UB has a model size that is 3 times lighter than the standard UNet, and the computation time is 20 % faster on the same hardware. After the Seq_UB architecture was developed, a quantitative measurement of the segmentation of X-ray images of Covid-19 patients was developed. This uses Eq. (2), which compares the total pixel value of a Covid-19 patient's image segmentation to the average total pixel of normal image segmentation. An interesting pattern was found, where Covid-19 patients quantitatively experienced fluctuations in image segmentation size.

Conclusions

Our research shows that the Seq_UB Architecture-based image segmentation method can reduce the computational burden with a segmentation accuracy of 96 % in segmenting thorax X-ray images of Covid-19 and pneumonia patients. The Seg_UB model has a light computational load of only 2,379,073 parameters, making the chest X-ray image segmentation process take an average of 0.91 s. The trained Model has been applied to a sequential X-ray image analysis system and enables quantitative analysis of X-ray images with an integrated approach. The Seq_UB is a promising architecture for accurate, fast, and lightweight X-ray image segmentation.

Acknowledgments

This research is funded by a Doctoral Research Grant from Brawijaya University, Indonesia in 2022.

References

[1] K Ismail, H Bensasi, A Taha, A Nazir, M Abdelkhalek, W Mohamed, D Lodhe, S Buschbeck, M Bauer and Y Sakr. Characteristics and outcome of critically ill patients with coronavirus disease-2019 (covid-19) pneumonia admitted to a tertiary care center in the United Arab Emirates during the first wave of the SARS-CoV-2 pandemic. A retrospective analysis. *PLos One* 2021; **16**, e0251687.

[2] D Wootton and C Feldman. The diagnosis of pneumonia requires a chest radiograph (x-ray)-yes, no or sometimes? *Pneumonia* 2014; **5**, 1-7.

[3] G Besutti, PG Rossi, M Ottone, L Spaggiari, S Canovi, F Monelli, E Bonelli, T Fasano, N Sverzellati, A Caruso, N Facciolongo, G Ghidoni, A Simonazzi, M Iori, A Nitrosi, S Fugazzaro, S Costi, S Croci, E Teopompi, A Gallina, ..., C Salvarani. Inflammatory burden and persistent CT lung abnormalities in covid-19 patients. *Sci. Rep.* 2022; **12**, 4270.

[4] S Waite, A Grigorian, RG Alexander, SL Macknik, M Carrasco, DJ Heeger and S Martinez-Conde. Analysis of perceptual expertise in radiology - current knowledge and a new perspective. *Front. Hum.*

Neurosci. 2019; **13**, 213.
[5] YMY Abdallah and T Alqahtani. *Research in medical imaging using image processing techniques*. *In*: Y Zhou (Ed.). Medical Imaging. IntechOpen, London, 2019.
[6] MAR Ahad, S Kobashi and JMRS Tavares. Advancements of image processing and vision in healthcare. *J. Healthc. Eng.* 2018; **2018**, 8458024.
[7] L Lu, X Wang, G Carneiro and L Yang. *Deep learning and imaging and clinical networks for medical convolutional neural informatics*. Advances in Computer Vision and Pattern Recognition. Springer Cham, Switzerland, 2019.
[8] M Xin and Y Wang. Research on image classification model based on deep convolution neural network. *EURASIP J. Image Video Process.* 2019; **2019**, 40.
[9] S Srivastava, AV Divekar, C Anilkumar, I Naik, V Kulkarni and V Pattabiraman. Comparative analysis of deep learning image detection algorithms. *J. Big Data* 2021; **8**, 66.
[10] S Minaee, YY Boykov, F Porikli, AJ Plaza, N Kehtarnavaz and D Terzopoulos. Image segmentation using deep learning: A survey. *IEEE Trans. Pattern Anal. Mach. Intell.* 2021; **44**, 3523-42.
[11] A Aggarwal, M Mittal and G Battineni. Generative adversarial network: An overview of theory and applications. *Int. J. Inform. Manag. Data Insights* 2021; **1**, 100004.
[12] VV Danilov, D Litmanovich, A Proutski, A Kirpich, D Nefaridze, A Karpovsky and Y Gankin. Automatic scoring of covid-19 severity in x-ray imaging based on a novel deep learning workflow. *Sci. Rep.* 2022; **12**, 12791.
[13] O Ronneberger, P Fischer and T Brox. U-net: Convolutional networks for biomedical image segmentation. Lect. *Notes Comput. Sci.* 2015, https://doi.org/10.1007/978-3-319-24574-4_28.
[14] CS Widodo, N Agus, MM Mahasin, Y Yueniwati, TA Putranto and PI Patra. UBNet: Deep learning-based approach for automatic x-ray image detection of pneumonia and covid-19 patients. *J. X Ray Sci. Tech.* 2021; **30**, 57-71.
[15] A Degerli, M Ahishali, M Yamac, S Kiranyaz, MEH Chowdhury, K Hameed, T Hamid, R Mazhar and M Gabbouj. Covid-19 infection map generation and detection from chest x-ray images. *Health Inform. Sci. Syst.* 2021; **9**, 15.
[16] S Jaeger, S Candemir, S Antani, YXJ Wáng, PX Lu and G Thoma. Two public chest x-ray datasets for computer-aided screening of pulmonary diseases. *Quant. Imag. Med. Surg.* 2014; **4**, 475-7.
[17] Y Tang, Y Tang, J Xiao and RM Summers. XLSor: A robust and accurate lung segmentor on chest x-rays using criss-cross attention and customized radiorealistic abnormalities generation. *arXiv* 2019, https://doi.org/10.48550/arXiv.1904.09229.
[18] H Zhao and F Cao. Automatic lung segmentation algorithm on chest x-ray images based on fusion variational auto-encoder and three-terminal attention mechanism. *Symmetry* 2021; **13**, 814.
[19] E Shelhamer, J Long and T Darrell. Fully convolutional networks for semantic segmentation. *IEEE Trans. Pattern Anal. Mach. Intell.* 2015; **39**, 640-51.
[20] M Abadi, A Agarwal, P Barham, E Brevdo, Z Chen, C Citro, GS Corrado, A Davis, J Dean, M Devin, S Ghemawat, I Goodfellow, A Harp, G Irving, M Isard, Y Jia, R Jozefowicz, L Kaiser, M Kudlur, J Levenberg, ..., X Zheng. TensorFlow: Large-scale machine learning on heterogeneous systems. *arXiv* 2015, https://doi.org/10.48550/arXiv.1603.04467.
[21] Keras, Available at: https://github.com/fchollet/keras, accessed March 2023.
[22] R Yasin and W Gouda. Chest x-ray findings monitoring covid-19 disease course and severity. *Egypt. J. Radiol. Nucl. Med.* 2020; **51**, 193.
[23] HJ Chen, SJ Ruan, SW Huang and YT Peng. Lung x-ray segmentation using deep convolutional neural networks on contrast-enhanced binarized images. *Mathematics* 2020; **8**, 545.
[24] Z Zhou, MR Siddiquee, N Tajbakhsh and J Liang. UNet++: A nested u-net architecture for medical image segmentation. *arXiv* 2018, https://doi.org/10.48550/arXiv.1807.10165.
[25] C Liang-Chieh, G Papandreou, F Schroff and H Adam. Rethinking atrous convolution for semantic image segmentation. *arXiv* 2017, https://doi.org/10.48550/arXiv.1706.05587.
[26] C Liang-Chieh, Y Zhu, G Papandreou, F Schroff and H Adam. Encoder-decoder with atrous separable convolution for semantic image segmentation. *arXiv* 2018, https://doi.org/10.48550/arXiv.1802.02611.
[27] A Kirillov and P Dollár. *A unified architecture for instance and semantic segmentation object detection vs semantic segmentation*. Universität Heidelberg, Germany, 2021.
[28] A Chaurasia and E Culurciello. LinkNet: Exploiting encoder representations for efficient semantic segmentation. *arXiv* 2017, https://doi.org/10.1109/VCIP.2017.8305148.
[29] H Zhao, J Shi, X Qi, X Wang and J Jia. Pyramid scene parsing network. *In*: Proceedings of the 2017 IEEE Conference on Computer Vision and Pattern Recognition, Hawaii. 2017.

[30] H Li, P Xiong, J An and L Wang. Pyramid attention network for semantic segmentation. arXiv 2018, https://doi.org/10.48550/arXiv.1805.10180.
[31] T Fan, G Wang, Y Li and H Wang. Ma-net: A multi-scale attention network for liver and tumor segmentation. *IEEE Access* 2020; **8**, 179656-65.